Experimental Study on the Effects of Turbulence and Ambient Composition on Butanol Droplet Evaporation

Perry Cheung, Arash Arabkhalaj and Madjid Birouk
Department of Mechanical Engineering, University of Manitoba
15 Gillson St., Winnipeg, Manitoba, Canada R3T 5V6

1 Introduction

The effects of ambient gases such as carbon dioxide, oxygen, and exhaust gas on droplet evaporation as an attempt to understand the impact of combustion products have been studied in the literature. However, these studies, which are mostly numerical, are very scarce. The following is a brief review of relevant literature. Markadeh and Ghassemi [1] simulated the effect of ambient oxygen presence (N_2/O_2) at 700 K and found that its effect depends on its concentration. Yi et al. [2] numerically investigated the effect of ambient oxygen at ambient temperatures below 700 K and found that the evaporation rate increases linearly with increasing oxygen concentrations. Yi et al. [2] simulated the effect of carbon dioxide (CO_2) in a nitrogen ambient (N_2/CO_2) and found that the evaporation rate increases with increasing CO_2 concentrations of up to 10%, after which it drops with further increase in CO_2. Zhang et al. [3] simulated the effects of ambient combustion gases ($N_2/O_2/H_2O/CO_2$) on the evaporation rate. They found that the evaporation rate increased with the increasing presence of polar molecules (H_2O). Yi et al. [2] also conducted simulations evaluating the effects of EGR on the evaporation rate of fuels and found that the evaporation rate is enhanced at EGR concentrations below 70% (N_2/EGR), and the degree of enhancement is higher for fuels with higher molecular weights. They investigated the evaporation rate at 465 K, 545 K, and 620 K, and found that molecular weight dependency decreases significantly at the tested highest temperature (620 K). The combined effects of EGR and pressure were also studied, and they reported that the enhancement effect of EGR on droplet evaporation is further increased at high pressures. Markadeh and Ghassemi [1] simulated the effects of adding EGR to air and a N_2/O_2 ambient, and found that the evaporation rate increases with EGR in air, while in a N_2/O_2 ambient, the addition of EGR decreased the evaporation rate at lower temperature range ($\sim<$ 500 K), whereas it increased at higher temperatures (600 - 1000 K). Radhakrishnan et al. [4] experimentally investigated the effect of ambient gas density on the evaporation rate and found that the droplet evaporation rate was lower in denser gases. Mazumder et al. [5] simulated the effect of ambient gas viscosity on evaporation rate and found that the droplet evaporation rate decreased with decreasing ambient gas viscosity. Both studies ([4, 5]) found that CO_2 had a lower evaporation rate than N_2.

Correspondence to: madjid.birouk@umanitoba.ca

As briefly reviewed above, published studies dedicated to this topic are mostly numerical simulations. While they provided valuable insights into droplet evaporation in multi-component ambient gases (e.g., CO_2, O_2, EGR), validation of these numerical findings requires experimental data. Additionally, studies on ambient CO_2 effects are particularly scarce and would benefit from further experimental investigation. Similarly, contrasting numerical results regarding the impact of ambient oxygen would benefit from experimental evidence. The varying ambient compositions in EGR studies (e.g., EGR/N_2/O_2, EGR/air, EGR) cause difficulties in comparisons, highlighting a need for a systematic experimental approach to allow for comparison. Furthermore, all these published numerical studies were conducted in quiescent environments, highlighting the opportunity to conduct experiments under turbulent conditions that better replicate in-engine conditions.

The objective of the present study is to experimentally investigate the effects of ambient gas composition in a turbulent environment on the evaporation rate of butanol droplets at standard atmospheric conditions.

2 Methodology

Single droplet vaporization experiments were conducted in a large fan-stirred spherical chamber. Butanol (99.9% purity) droplets with a diameter of 500 μm ($\pm$5%) were evaporated in multi-component atmospheres at 27 $\pm$1°C and 1 bar. Ambient flow conditions ranged from stagnant to turbulent conditions with fan speeds ranging from 0 - 3000 RPM, corresponding to turbulence intensities of 0 - 1.5 m/s. Table 1 summarizes the single, binary, and triple ambient gas compositions tested in this study. Detailed descriptions of the experimental methodology have been documented in previous works by our research group (e.g., [6, 7]), with key aspects summarized in the following.

Table 1: Tested single, binary, and triple ambient gas compositions.

Single Composition	Binary Composition	Triple Composition
100% N_2	50% O_2 - 50% N_2	50% N_2 - 25% O_2 - 25% CO_2
100% CO_2	50% O_2 - 50% CO_2	50% CO_2 - 25% O_2 - 25% N_2
100% O_2	50% CO_2 - 50% N_2	50% O_2 - 25% CO_2 - 25% N_2

The experiment is conducted in a 29-liter stainless steel fan-stirred spherical chamber with four coaxially paired fans used to generate a homogenous and isotropic turbulent flow field inside the chamber. Two crossed 14 μm Hi Nicalon silicon carbide (SiC) fibers are attached to an aluminum frame for use in the cross fiber technique. This technique has been demonstrated to promote droplet sphericity, mitigate heat conduction through the suspension system, and support a wide range of droplet sizes (e.g., [7, 8, 9]). Butanol droplets are created using a hand-operated fuel injector which is capable of generating a wide range of droplet sizes ranging from around 100 μm to 1000 μm through a capillary tube with an inner and an outer diameter of 40 μm and 60 μm, respectively. Dantec Dynamics 2D-PIV system is used to characterize the turbulent flowfield inside the spherical chamber. The main components of this PIV system are a Dual Power Nd:YAG laser (135 mJ double pulse), a FlowSense EO 4 M camera, and DynamicStudio software. The flow is seeded with olive oil micro-droplets generated by a LaVision aerosol generator. PIV characterization revealed that the flowfield inside the chamber is isotropic and homogeneous with a nearly zero-mean velocity component. Turbulence intensity, expressed as the square root of the turbulent kinetic energy, $q^{1/2}$, varies with the fan's speed as $q^{1/2} = 0.0005 * N$. Detailed PIV test results are reported in [8]. To capture the vaporization process of the butanol droplet, a Fastec IL5Q camera paired with a Questar QM-100 long-distance microscope is utilized with a halogen lamp as a

backlight source. The droplet images taken are then processed using an in-house MATLAB code to determine the average evaporation rate, $\overline{K}$. The systematic error involved in determining the droplet size is a result of camera calibration and the droplet edge detection algorithm. The camera calibration included measuring the diameter of a known object, with an estimated uncertainty of approximately 1%. Droplet edge detection was evaluated by comparing two different thresholds (Otsu and an artificially high value), which resulted in an initial diameter (d_0) calculation difference of less than 2%. The uncertainty in determining the droplet vaporization rate was assessed by repeating each experimental condition at least four times and applying a 95% confidence interval. Calculations indicated that the standard error was less than 5% across all tested conditions.

3 Results and Discussion

The temporal variation of the normalized droplet squared diameter at different test conditions is shown in Figure 1. This figure clearly exhibits a linear variation, validating the application of the d^2-law under all tested conditions. Figure 2 illustrates the variation of the average evaporation rate of a butanol droplet as a function of turbulence intensities for different pure ambient conditions (i.e., N_2, O_2, and CO_2). This figure reveals the similarities between the evaporation rates of N_2 and O_2, and highlights the significant evaporation rate decrease in pure CO_2 for all tested turbulence intensities. The comparable thermophysical properties of N_2 and O_2 is likely the main reason for their similar evaporation rates.

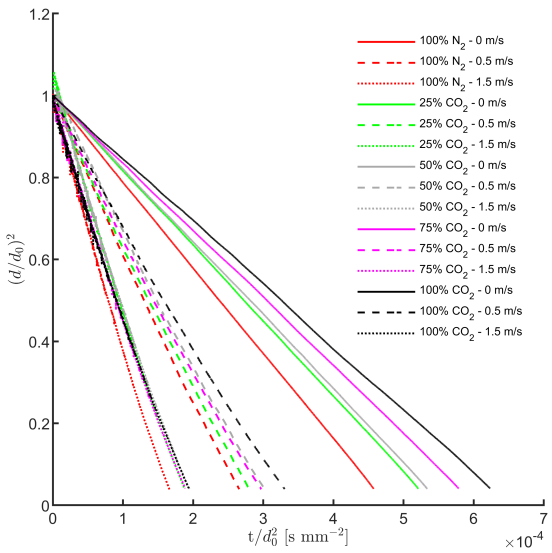

Figure 1: Temporal variation of the normalized butanol droplet squared diameter under different turbulence intensities for different CO_2 concentrations.

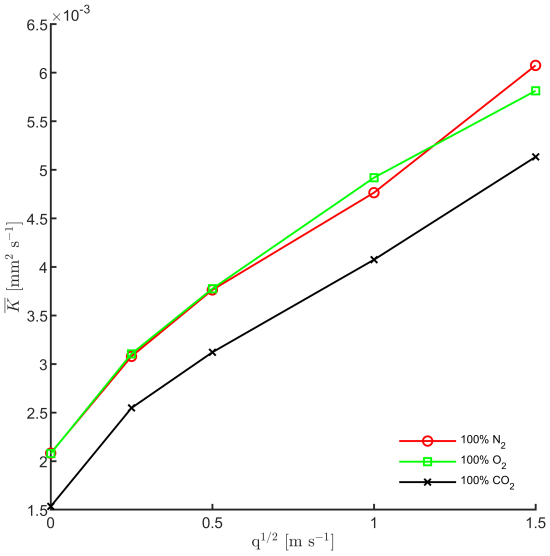

Figure 2: Variation of butanol droplet evaporation rate with turbulence intensity in 100% N_2, O_2, and CO_2.

Figure 3 illustrates the variation of the average evaporation rate of a butanol droplet as a function of turbulence intensity for different ambient CO_2 concentrations in N_2. This figure reveals that the droplet evaporation rate increases with turbulence intensity regardless of the ambient gas composition. More importantly, this figure shows that, at any turbulence intensity, the droplet evaporation rate decreases with increasing the concentration of CO_2 in the ambient gas.

Figure 4 illustrates the variation of the droplet average normalized evaporation rate as a function of turbulence intensity for all tested binary N_2-CO_2 combinations. The normalized average droplet evaporation rate, $\overline{K}/\overline{K_0}$, is calculated by dividing the averaged evaporation rate at each turbulence intensity with the evaporation rate under stagnant conditions, $\overline{K_0}$, at the same ambient composition. This figure demonstrates that the butanol droplet normalized evaporation rate increases with the concentration of CO_2 in the ambient gas, and this is valid at all tested turbulence intensities. The fact that droplet evaporation increased with turbulence intensity when increasing ambient carbon dioxide gas concentration is an indication that turbulence effectiveness is more pronounced at higher ambient carbon dioxide concentrations.

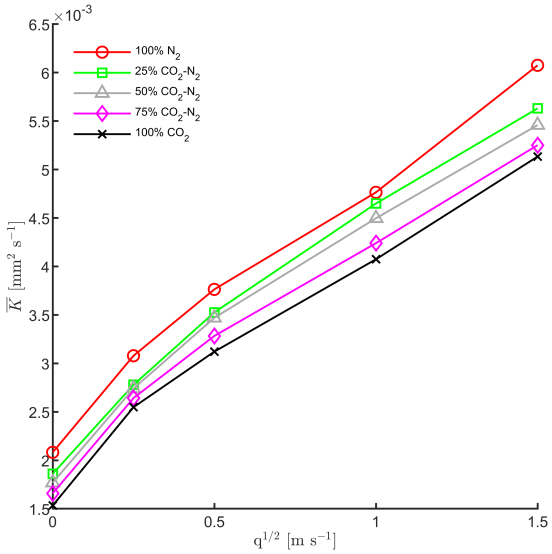

Figure 3: Variation of butanol droplet evaporation rate with turbulence intensity for different ambient CO_2 concentrations.

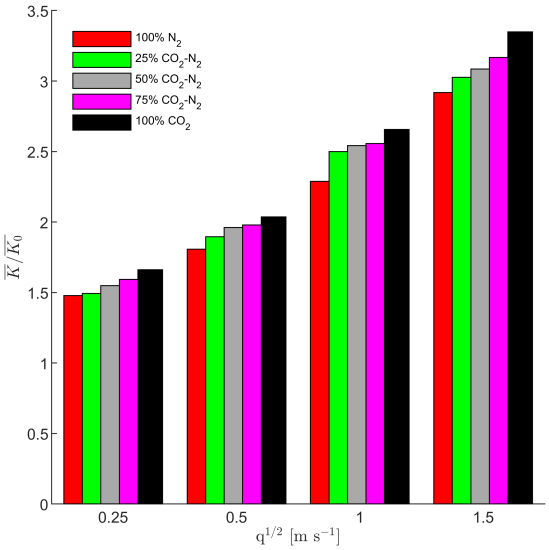

Figure 4: Butanol normalized evaporation rate as a function of turbulence intensity for different ambient CO_2 concentrations.

The effects of ambient binary compositions containing O_2 and triple compositions containing N_2-O_2-CO_2 on the average evaporation rate is presented in Figure 5. This figure shows that the evaporation rate in 100% N_2 and 100% O_2 is similar, with that of CO_2 being significantly lower at all turbulence intensities as is already shown in previous figures. Also, the average evaporation rate of the binary compositions containing CO_2 is also lower compared to its counterpart combination of O_2 and N_2 (i.e., 50% O_2-N_2). As for the triple ambient composition cases, the average evaporation rate of 50% O_2-25% CO_2-N_2 is the highest, followed by 50%N_2-25% O_2-CO_2, and then 50% CO_2-25% O_2-N_2 being the lowest at all turbulence intensities except 1.5 m/s.

Figure 6 shows the variation of the normalized vaporization rate as a function of turbulence intensity in an ambient of binary or triple composition containing O_2. Both 100% N_2 and O_2 ambient gas exhibit similar droplet evaporation rate enhancement by turbulence. The binary combination, 50% O_2-N_2, demonstrates similar turbulence enhancements to 100% N_2 and O_2, with a decreased turbulence effectiveness compared to binary combinations with CO_2. Turbulence effectiveness of all triple ambient compositions was similar, with 50% O_2-25% CO_2-N_2 having a slightly lower evaporation rate enhancement at the highest turbulence intensity of 1.5 m/s.

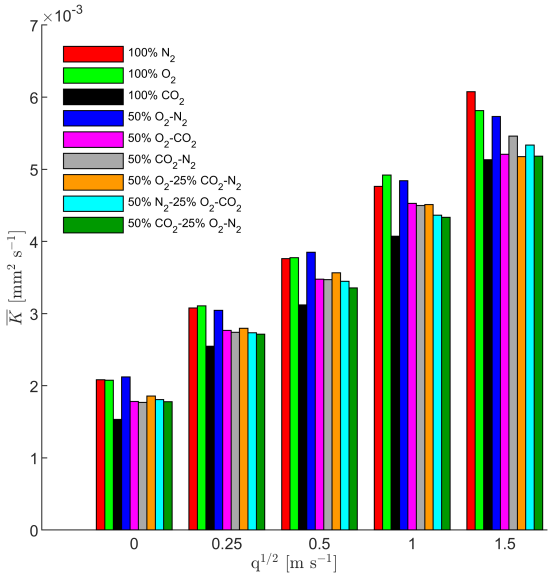

Figure 5: Butanol droplet evaporation rate variation with turbulence intensity for different ambient compositions of N_2-CO_2-O_2.

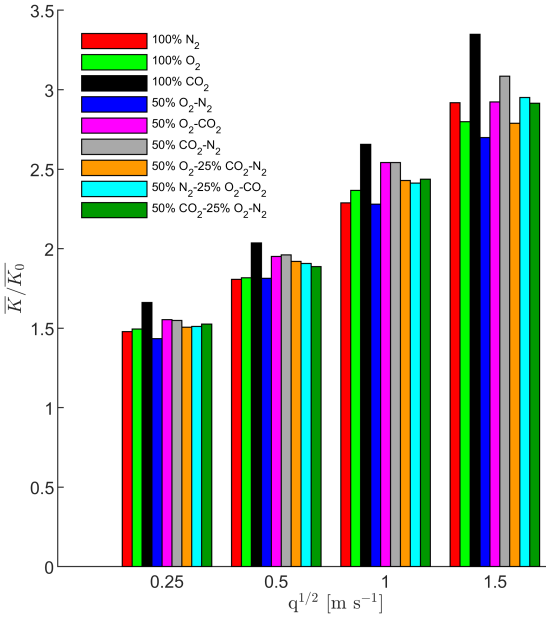

Figure 6: Butanol droplet normalized evaporation rate variation with turbulence intensity for different ambient compositions of N_2-CO_2-O_2.

4 Concluding Remarks

The experimental results demonstrated that $\overline{K}$ increased with turbulence intensity regardless of the ambient gas composition. However, the evaporation rate varied differently with the ambient gas composition. For single-component ambient gases (N_2, CO_2 or O_2), $\overline{K}$ in N_2 and O_2 was comparable, while CO_2 exhibited a significantly lower $\overline{K}$ across all turbulence intensities. As for the binary 50%-50% gas compositions (O_2-N_2, O_2-CO_2 or CO_2-N_2), O_2-N_2 showed a noticeably higher $\overline{K}$ compared to the other two CO_2 containing combinations. In the two binary combinations containing CO_2, $\overline{K}$ was similar under all turbulence intensities except at 1.5 m/s, where CO_2-N_2 was slightly higher. Additionally, $\overline{K}$ consistently decreased with increasing CO_2 concentrations at all turbulence intensities. Lastly, for triple (N_2-CO_2-O_2) ambient compositions (50%-25%-25%), $\overline{K}$ was overall comparable, with 50% O_2-25% CO_2-N_2 exhibiting a slightly higher value at all turbulence intensities except at the highest tested turbulence intensity (1.5 m/s).

Using the normalized average evaporation rate ($\overline{K}/\overline{K}_0$) as an indicator of turbulence effectiveness, the results showed that while the single-component gases (N_2 and O_2) showed similar turbulence effectiveness, CO_2 exhibited the greatest overall turbulence effectiveness. As for the 50%-50% binary compositions, O_2-N_2 had lower turbulence effectiveness compared to its counterparts containing CO_2 which both showed comparable turbulence effectiveness. For the tested binary CO_2 combinations, turbulence effectiveness was more pronounced at higher ambient CO_2 concentrations. Lastly, turbulence effectiveness was similar for the three triple ambient combinations, with 50% O_2-25% CO_2-N_2 showing a slight decrease in turbulence effectiveness at the highest turbulence intensity of 1.5 m/s.

Further work is underway to enable testing at higher turbulence intensities in order to investigate the change of trend exhibited in the present results.

5 Acknowledgements

This research was supported by the Natural Sciences and Engineering Research Council of Canada (NSERC).

References

[1] Markadeh R. S, Ghassemi H. (2018). A discrete multicomponent droplet evaporation model; effects of o2-enrichment, steam injection, and egr on evaporation of diesel droplet. Numerical Heat Transfer, Part A: Applications, 73(10):721–742.

[2] Yi P, Feng L, Jia M, Long W, Tian J. (2014). Development of an improved multi-component vaporization model for application in oxygen-enriched and egr conditions. Numerical Heat Transfer, Part A: Applications, 66(8):904–927.

[3] Zhang K, Ma X, Gong Y, Li Y, Wang Z, Jiang C, Shuai S. (2024). A molecular dynamics study on supercritical evaporation of ammonia droplets in multi-component environments. Journal of Molecular Liquids, 394:123808.

[4] Radhakrishnan S, Anand T. N. C, Bakshi S. (2019). Evaporation-induced flow around a droplet in different gases. Physics of Fluids, 31(9):092109.

[5] Mazumder N. S, Lingfa P, Neog C. K. (2023). Evaporation characteristics of ethanol droplet in different gases under force convection condition. Engineering Research Express, 5(1):015005.

[6] Verwey C, Birouk M. (2017). Experimental investigation of the effect of droplet size on the vaporization process in ambient turbulence. Combustion and Flame, 182:288–297.

[7] Verwey C, Birouk M. (2020). Experimental investigation of the evaporation of suspended monosized heptane droplets in turbulence intensities approaching unity. Combustion and Flame, 219:425–436.

[8] Arabkhalaj A, Verwey C, Birouk M. (2023). Experimental study of butanol droplet evaporation in a turbulent, high-pressure environment. Fuel, 353:129143.

[9] Arabkhalaj A, Verwey C, Birouk M. (2024). Experimental investigation of the effect of droplet size on the vaporization of butanol in turbulent environments at elevated pressure. International Journal of Heat and Mass Transfer, 226:125525.